

## The Potential Histological Effect of Experimental Obesity on The Liver of Male Albino Rats (Light and Electron Microscopic Study)

Ahmad Mohammad Abdel-Aleem Desoky

Histology Department - Faculty of Medicine - Al-Azhar University - Assiut - Egypt

E mail: dr.ahmad.abdel.aleem@azhar.edu.eg Tel: Tel: 002 01155988640,

Orcid no.: 0000-0001-8543-7102

### ABSTRACT

**Background:** There is a growing global awareness to the hazards of obesity. The obese patients are much more liable to many serious diseases including liver failure.

**The aim of work:** was to study light and electron microscopic changes of the liver, as well as, the liver enzymes in the experimentally obese albino rats.

**Methodology:** Sixty male albino rats were divided to 3 groups: **1- control group:** was fed standard laboratory diet for 4 weeks. **2- Obese group:** were given one intraperitoneal injection of Triton WR 1339 to induce obesity and fed normal laboratory diet for 4 weeks. **3- Recovery group:** similar to obese group but left for additional 4 weeks for recovery. The weights of animals were recorded, blood samples were collected for liver enzymes (ALT, AST and GGT) and the livers were weighted. Liver samples were fixed in glutaraldehyde for EM examination; and other samples were fixed in 10% formol saline then stained by H&E, Mallory trichrome and PAS stains for LM examination.

**Results:** Obese animals had significantly higher body weights, liver weights, and liver enzymes than the control group. Histologically, there was a non-significant increase in the collagen area of obese group. There was a highly significant reduction in the optical density of glycogen in the obese group. However, the optical density in the recovery group was lower than that of control group. **Conclusion:** obesity may induce several abnormal changes in the hepatocytes, and inflammation similar to steatosis or steatohepatitis.

**Keywords:** liver - triton - obese – Obesity - albino rats.

### INTRODUCTION

Obesity is a global disorder that impacts both developed and developing countries; it represents the world's second reason for preventable death <sup>(1)</sup>. According to the WHO, obesity has nearly tripled since 1975; in 2016 over 650 million adults were obese, counting approximately 13% of the total population. Additionally, 39 million children under five years were overweight or obese worldwide in 2020 <sup>(2)</sup>. High-fat and high-cholesterol diets cause increased cholesterol and triglycerides in blood, both of which cause oxidative stress which is a major factor in the development of nonalcoholic fatty liver disease <sup>(3)</sup>. Today, oxidative stress is one of the major health threats; it became the medical and nutritional puzzle for the twenty first century <sup>(4)</sup>. Non-alcoholic fatty liver disease, being the most common liver disorder worldwide, is affected by obesity. Its prevalence ranges from seventy to ninety percent <sup>(5)</sup>. It is characterized by triacylglycerol accumulation inside liver cells. It can progress to more dangerous conditions, such as non-alcoholic steatohepatitis, liver fibrosis and liver cirrhosis, and in rare cases, liver carcinoma <sup>(6)</sup>. This work was performed to study the light and electron microscopic changes, as well as enzymatic changes in the liver caused by Triton-induced obesity in male albino rats as a model of experimental obesity.

### MATERIAL AND METHODS

This research was carried out at Al-Azhar University's Faculty of Science in Cairo, Egypt. All

experimental procedures were carried out according to the principles and guidelines of Ethics Committee of Faculty of Science at Al-Azhar University – Cairo, Egypt, and according to "Guide for care, and use of experimental laboratory animals" issued by US National Institute of Health for use and welfare of experimental animals <sup>(7)</sup>.

In this study, sixty male albino rats weighing 120 ± 5 grams and ranging from 4-5 weeks in age were used. Rats were housed in 6 clean metallic cages with metallic mesh cover that measured

120 X 60 X 60 cm containing ten rats in each cage. Animals were fed standard laboratory diet with plenty of water to ensure normal growth. All animals were housed for 1 week prior to our study for acclimatization with the current conditions. Every week, the weight of animals was recorded. The 60 male albino rats were divided into 3 groups, each group consisted of twenty rats, as follows:

**Group I (Control group):** twenty rats were fed standard laboratory diet for four weeks before being sacrificed. This group served as a negative control.

**Group II (Obese group):** Twenty rats were given intraperitoneal injection of Triton 250 mg/kg to induce obesity <sup>(8)</sup> then fed normal laboratory diet for 4 weeks before being sacrificed. This group served as a positive control.

**Group III (Recovery group):** twenty rats were treated as group II but were left for additional 4 weeks (to allow for spontaneous recovery) before being sacrificed.

Triton WR 1339 (Tyloxpole)<sup>®</sup> was purchased from Sigma-Aldrich U.S.A in the form of vials 50 ml containing 50 grams of triton. Triton was dissolved in the normal saline to make solution at concentration equal 100 mg/ml (1 ml of triton/9 ml of normal saline). Triton was given by intra-peritoneal (IP) injection in dose of 250 mg/kg (i.e. 0.25 ml of the prepared solution/100 grams body weight) according to *Walaa and Saad* <sup>(8)</sup>. The intraperitoneal (IP) injection is the most commonly used parenteral route of administration in rats due to the large surface area of the abdominal cavity. The peritoneum is also associated with abundant blood supply which allow for rapid absorption. Absorption via this route is typically half to one-quarter as fast as that via intravenous route <sup>(9)</sup>.

Triton was administered intraperitoneally as follows: At the beginning, the abdomen can be divided into four quadrants by the midline and a line perpendicular to it passing through the umbilicus. Intraperitoneal injections should be given into the lower left quadrant of the abdomen. In this area of the rat there are no vital organs except for the small intestine. In contrast, the lower right quadrant contains much of the large bowel, and the upper abdomen is a hazardous area to inject because the liver, stomach and spleen are situated here. The needle must be inserted along this line on animal's right side, close to middle line. This is less likely to puncture the small intestines. If the needle is inserted too much caudally or laterally from insertion point mentioned above, injection into right leg may occur, injuring muscle tissue of the animal. Second, we do IP injection while the rat was restrained and unable to move during the procedure to prevent organs from being traumatized once needle has entered abdomen. The rat was tilted so that its head was facing down while his abdomen was revealed. After disinfecting the injection site, the needle was inserted into the abdomen at thirty-degree angle. The needle should be inserted about half centimeter depth. We aspirate to ensure that the needle has not entered intestines, urinary bladder or blood vessels. If any fluid was aspirated, solution must be discarded, and the procedure must be repeated using a new syringe. It is possible to inject triton if no fluid is aspirated.

**Determination of liver enzymes:** At the end of the experiment, blood samples were taken from retroorbital plexus of all rats under diethyl ether anesthesia before decapitation and after overnight fasting. Blood samples were then collected in clean dry Wassermann tubes without anticoagulant then left to clot at room temperature in slope position. The tubes were centrifuged at 3000 rpm for five minutes. Serum of non-hemolyzed samples was thoughtfully transferred into clean dry Eppendorf tubes

that were kept frozen at -20°C till used for biochemical analysis. Kits for liver function tests (ALT, AST and GGT) were purchased from Vitro Scient Company while the histological stains were purchased from El-Gomhoria company for chemicals, Mansoura, Egypt. The stains included hematoxylin and eosin, Mallory trichrome and PAS stains.

**Electron microscopic study:** after anesthesia, blood sampling and decapitation were done; the abdomen and chest were opened longitudinally, then while the heart was beating a 12 gauge canula was inserted in the right ventricle and a small incision in the right atrium was done using scalpel, to infuse a solution of normal saline containing 2.5 % glutaraldehyde and one ampule of heparin directly in the heart to infuse the rat tissue with the fixative to avoid any destruction or changes in the ultrastructure of their cells. Immediately after perfusion of the fixative, the livers were excised and a small piece was cut (from each liver) as a small cube about 1 × 1 × 1 mm in a dish containing 2.5 % glutaraldehyde solution, then placed in a small plastic pipe filled with 2.5 % glutaraldehyde.

According to *Mark et al.* <sup>(10)</sup>, the tissue was transferred to osmium tetroxide which has a strong reaction with membrane's lipids and proteins. After that, the sample was embedded by infiltrating it with resins capable of polymerizing into hard plastic appropriate for thin sectioning. Then, it was transferred to a tissue capsule that was ready for cutting and staining for EM examination. Toluidine blue staining of semithin sections (0.5 - 1.0 μm) was used as a guideline for further trimming (reagents: 1% Toluidine Blue plus two percent borate in distilled water). Ultrathin sections, (40 - 100 nm) were spread on 300 mesh copper grids and stained with uranyl acetate then lead citrate to improve image quality.

**Light microscopic study:** after decapitation, and evisceration under diethyl ether anesthesia, the liver was removed, samples were excised and washed by normal saline to remove blood, and then fixed in 10% formol saline. After putting the tissues in the fixative (10% formol saline) for 24 hours, fixed tissues were washed in a running tap water to remove the fixative from them, dehydration was done gradually in ascending grades of alcohol followed by clearing of the tissues. Then placed in molten soft paraffin in 50°C oven for 24 hours before being transmitted to molten hard paraffin in 55°C oven for 1 hour. Specimens were then placed in casts of molten hard paraffin. Casts and their contents were cooled in ice until paraffin solidified completely, forming blocks of hard paraffin.

Each block was cut into thin sections (5 μm) by rotatory microtome. Paraffin sections representing all groups were then placed on clean glass slides smeared with albumin glycerin. The slides were warmed on a hot plate then left for several hours in the incubator to dry<sup>(11)</sup> and finally stained by: Hematoxylin and eosin stain (to study general structure of the liver), Mallory trichrome stain (to study the distribution of collagen fibers in the liver) and PAS stain (to study glycogen content of the liver). Image analysis was done using Optimas software (version 6.2.1, Media Cybernetics, USA) to measure percentage of collagen area outside hepatocytes and optical density of glycogen inside hepatocytes.

**Statistical analysis**

After measuring means, standard errors, and P-value of the following parameters: body weight and liver weight, liver function tests (ALT, AST and GGT) and percentage of collagen area outside hepatocytes and optical density of glycogen inside hepatocytes. To determine impact of obesity on liver enzyme variables, ANOVA (one-way analysis of variance) was used, with Tukey post-hoc test for multiple comparisons. Collagen area and optical density variables either raw or transformed have violated the assumptions necessary to run the analysis of variance (normality of data and homogeneity of variances). Therefore, non-parametric alternative Kruskal-Wallis test was used, accompanied by pairwise comparison using Mann Whitney U test with Bonferroni correction. SPSS software (version 22; IBM Inc., Chicago, Illinois, USA) was used for analyses. The possibility of 0.05 or less was considered significant.

**RESULTS**

**Behavior and appetite:** During Triton injection period, rats were calm and easy to handle, with no injuries or deaths. The obese group's appetite was greater than control group, since evidenced by increased consumption (about 20 grams/ rat/ day for obese group and 14 grams /rat /day for control group). The appetite of recovery group decreased (about 17 grams /rat /day). There were no visible changes in both skin and hair.

**Body weight and liver weight:** The obese group gained weight at faster rate (up to 70 grams a week), while the control group gained weight at slower rate (around 30 grams a week). After discontinuing triton, the recovery group began to lose weight (around 10 grams a week). The results observed in tables (1 & 2) and charts (1 & 2) showed that there was a significant rise in body weight and liver weight of animals in the obese group when compared to the control group. Also, there was a significant reduction of body weight and liver weight in recovery group compared to obese group.

**Table (1):** Comparison between means, standard errors & P value of body weight in all groups

| Groups   | Mean of body weight (grams) |
|----------|-----------------------------|
| Control  | 242 ± 04.37 <sup>c</sup>    |
| Obesity  | 358 ± 10.70 <sup>a</sup>    |
| Recovery | 318 ± 08.15 <sup>b</sup>    |

Means with altered superscript vary significantly (P<05). (a) High value - (d) Low value - (b) and (c) In between

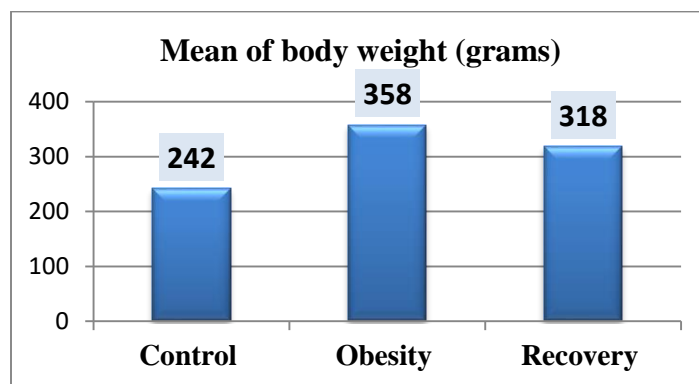


**Chart (1):** Comparison between means of body weight in various groups

**Table (2):** Comparison between means, standard errors & P value of liver weight in all groups

| Groups   | Mean of liver weight (grams) |
|----------|------------------------------|
| Control  | 04.54 ± 0.14 <sup>d</sup>    |
| Obesity  | 11.90 ± 0.21 <sup>a</sup>    |
| Recovery | 07.04 ± 0.13 <sup>b</sup>    |

Means with altered superscript vary significantly (P<05). (a) High value - (d) Low value - (b) and (c) In between

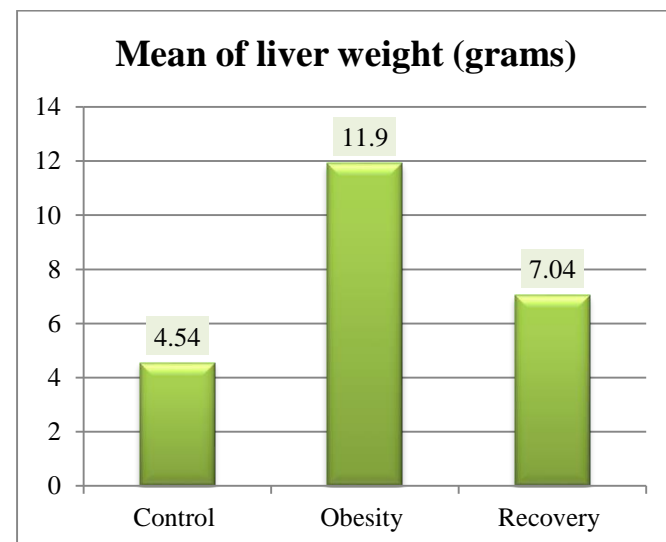


**Chart (2):** Comparison between means of liver weight in various groups

**Biochemical results:** The results observed in table-3 and chart-3 revealed that there was a significant rise in liver enzymes (ALT, AST and GGT) in the obese group when compared to the control group. As regard to recovery group, there was a significant improvement in the level of these enzymes when compared to obese group.

**Table (3):** Comparison between means, standard errors & P value of liver enzymes in all groups

| Groups   | Mean of ALT (U/l)         | Mean of AST (U/l)          | Mean of GGT (U/l)         |
|----------|---------------------------|----------------------------|---------------------------|
| Control  | 19.96 ± 1.38 <sup>c</sup> | 30.00 ± 1.23 <sup>c</sup>  | 5.89 ± 0.59 <sup>c</sup>  |
| Obesity  | 84.76 ± 3.56 <sup>a</sup> | 172.10 ± 9.22 <sup>a</sup> | 25.60 ± 1.55 <sup>a</sup> |
| Recovery | 42.10 ± 2.55 <sup>b</sup> | 072.70 ± 4.70 <sup>b</sup> | 13.00 ± 0.70 <sup>b</sup> |

Means with altered superscript vary significantly (P<05).

(a) High value - (d) Low value - (b) and (c) In between

ALT: Alanine aminotransferase enzyme.

AST: Aspartate aminotransferase enzyme.

GGT: Gamma glutamyl transferase enzyme.

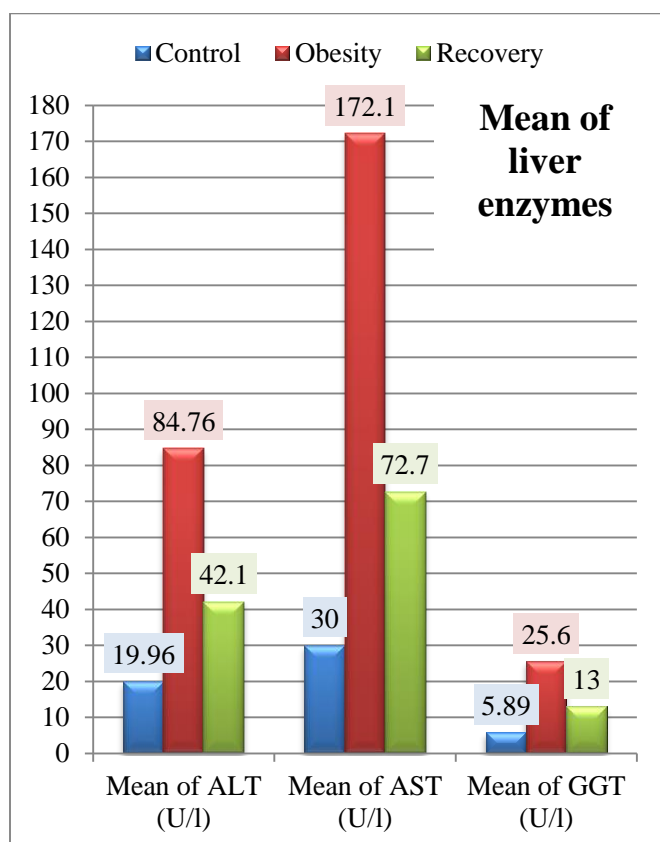


**Chart (3):** Comparison between means of liver enzymes in various groups

**Light microscopic results:** Examination of sections obtained from the liver of control group animals and stained by hematoxylin and eosin revealed classic hepatic lobules with nearly hexagonal shape. Its central vein forms a central axis and rows of liver cells are arranged in the form of radiating cords. Portal areas at the angles showed connective tissue stroma and portal triads. Hepatocytes are separated from one another by narrow blood sinusoids. Blood sinusoids were lined by endothelial cells and Kupffer cells. The hepatocytes were polygonal (in shape) containing rounded euchromatic nuclei "figure 1A and 1B".

On the other hand, the obese group showed many histological variations such as loss of cellular details and hyper-eosinophilic cytoplasm. There was also marked congestion and dilatation of portal veins, blood sinusoids and central veins were seen with rupture of endothelial lining of these blood vessels. In addition, cellular infiltrations were visible around central veins, around and in-between parts of portal tract and sometimes between hepatocytes. Hemolysis of RBCs inside blood vessels, increased Kupffer cells and fatty cells were also detected. Most of the hepatocytes exhibited marked enlargement by multiple variable-sized vacuoles (most probably lipid inclusion) that distend the cytoplasm, some had multiple small vacuoles, while others had single large vacuole with compressed peripheral nuclei. Furthermore, there was nuclear changes like darkly stained (pyknotic) nuclei, fragmented nuclei (karyorrhexis), and lysed nuclei (karyolysis) were noted "figure 1C and 1D".

Histological sections of recovery group showed slightly disturbed hepatic lobules with loss of cord architecture as well as presence of wide space between cords filled with erythrocytes and eosinophilic materials. Hepatocytes with multiple small and discrete vacuoles (possibly lipids) were seen in diverse zones of hepatic lobules in addition to hyper-eosinophilic cytoplasm and pyknotic nuclei in some cases. Moderate dilatation and congestion of central veins, portal veins and blood sinusoids were also reported with focal areas of mononuclear cellular aggregation (mainly lymphocytes and macrophages). However, the endothelial lining of central vein was intact with large flat nuclei "figure 1E and 1F".

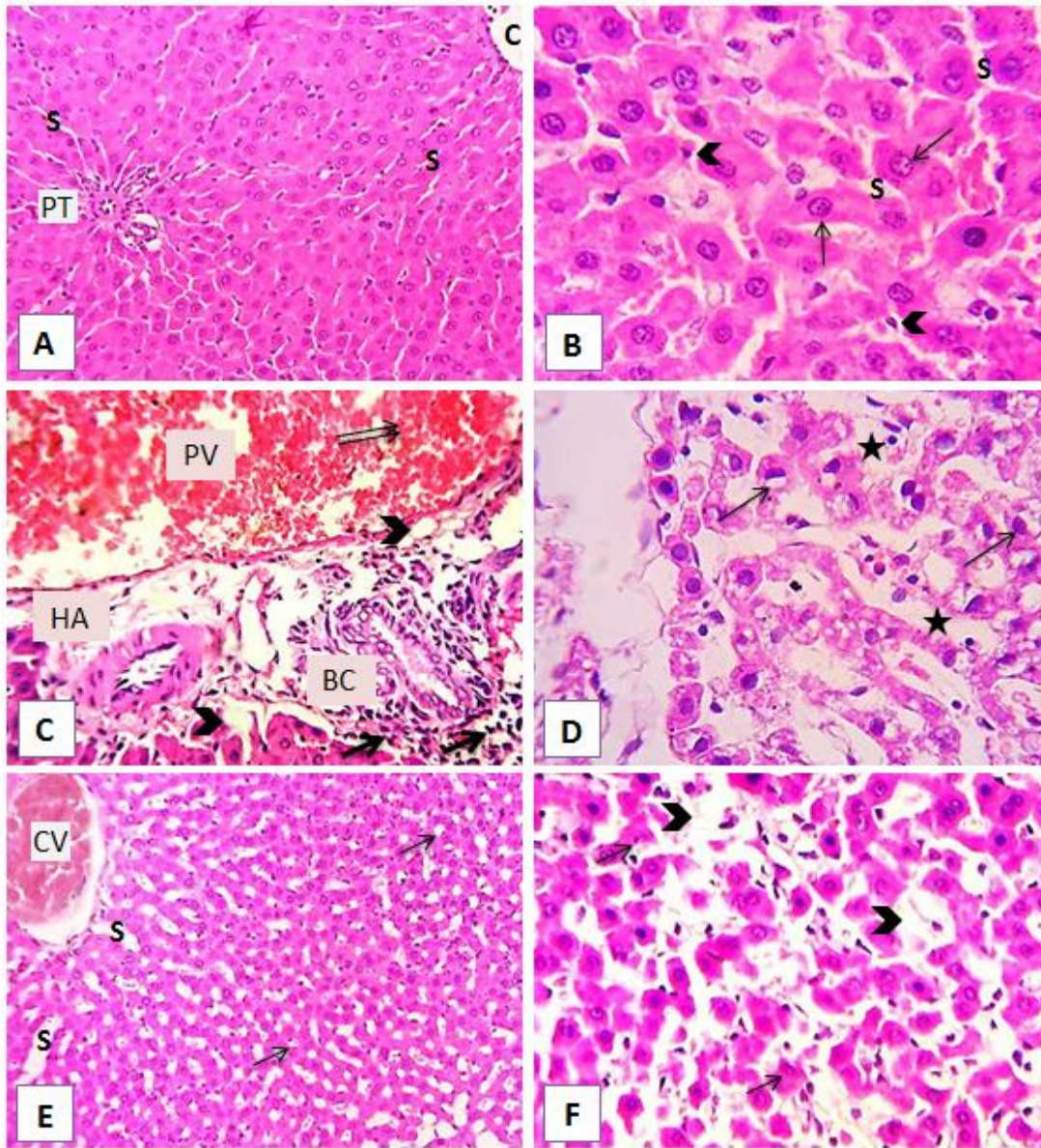


**Figure (1):** Photomicrographs of liver sections obtained from various experimental groups and stained by Haematoxylin and Eosin stains. **(A):** Liver section of control group demonstrated normal structure of classic hepatic lobules contained central vein "C" and radiating cords of hepatocytes. Blood sinusoids "S" existed among hepatocytes. Portal venule, hepatic arteriole and bile ductule were seen in portal tract "PT" at the periphery of classic hepatic lobules (200x). **(B):** Hepatocytes of control group were polygonal in shape and have rounded large euchromatic nuclei with prominent nucleoli "arrows." Flattened endothelial cells and Kupffer cells "arrow heads" were lined blood sinusoids "S" (1000x). **(C):** liver section of obese group showed highly disturbed portal area with marked congestion and dilatation of portal vein "PV" that contained hemolyzed RBCs "double arrow". Hepatic arteriole "HA" and bile canaliculus "BC" were surrounded by many lymphocytic infiltrations "thick arrows" and fat cells "arrow heads" (1000x). **(D):** liver section showing hepatocytes of obese group have vacuolated cytoplasm pushing their nuclei to the periphery "thin arrows" with widening of space of Disse "stars" (1000x). **(E):** liver section of recovery group showing normal histological structure with some fat vacuoles in most of hepatocytes "arrows". Dilated blood sinusoid "S" and dilated congested central vein "CV" with hemolyzed RBCs inside it were also noticed (200x). **(F):** Hepatocytes of recovery group lost their cord architecture with wide spaces between hepatic cords "arrow heads". Shrunken hepatocytes with pyknotic nuclei (arrows) were also observed (1000x).

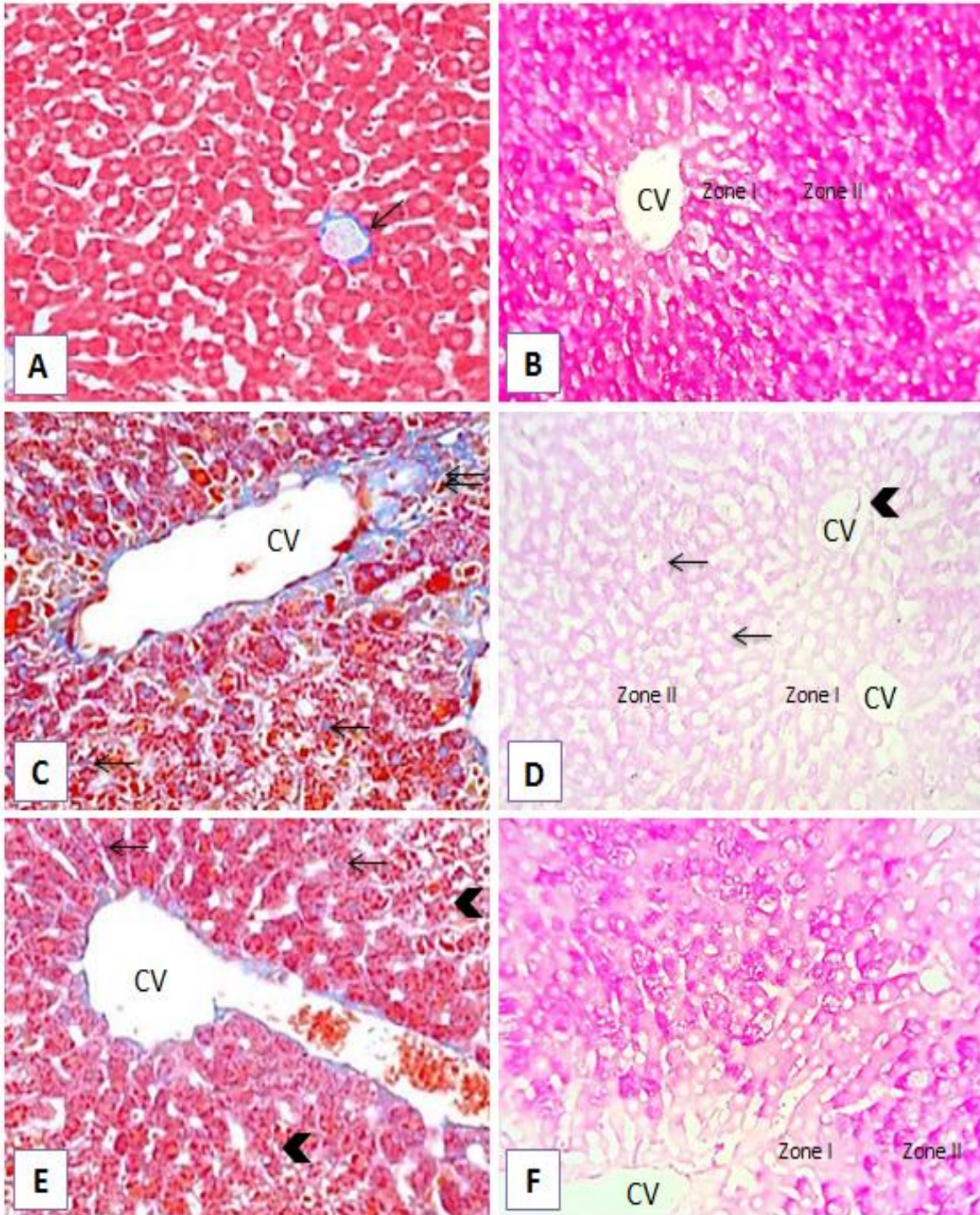


**Figure (2):** Photomicrographs of liver sections obtained from various experimental groups and stained by Mallory's trichrome stain (Left column) and PAS stain (Right column). **(A):** Liver section of control group demonstrated normal distribution of collagen fibers in the form of fine collagen bundles supporting central vein (arrow) (400x). **(B):** Hepatocytes of control group showed normal glycogen distribution around central vein (CV) in zones I and II (200x). **(C):** Liver section of obese group showing increased collagen fibers in most of liver tissues and condensed around dilated central vein (double arrow) and extending between cords of hepatocytes (arrows) (400x). **(D):** Hepatocytes of obese group are depleted from glycogen (marked PAS reduction) especially around central veins (CV) in zones I. The central vein showed endothelial detachment (arrow head) (200x). **(E):** Liver section of recovery group showed collagen fibers around dilated congested central vein (CV) and extended between hepatic cords (arrows). Hepatocytes showed small cytoplasmic (possibly fat) vacuoles (arrow heads) (400x). **(F):** Hepatocytes of recovery group demonstrating moderate stain affinity to glycogen around central vein (arrows) more in zone II like that of control group (400x).

Examination of liver sections of the control rats stained by Mallory’s trichrome stain, showed normal distribution of fine collagen fibers in the wall of both central veins and portal tracts. Collagen fibers were light blue; the nuclei were red while the smooth muscles were violet. Furthermore, examination of liver sections stained with Periodic acid-Schiff (PAS) of the control rats showed normal glycogen distribution in central areas and portal areas of the liver lobules with increased staining affinity. The glycogen appeared acidophilic or magenta and the basement membranes appeared also red "figure 2A and 2B".

However, examination of sections, obtained from liver of obese group and stained by Mallory’s trichrome stain, revealed slight rise in quantity of collagen fibers around central veins, blood sinusoids as well as around and in-between the components of portal tracts. Furthermore, examination of PAS-stained liver sections of this group showed highly depleted glycogen content from the hepatocytes in all zones of hepatic lobules with marked reduction in the staining affinity of the liver tissue "figure 2C and 2D".

Finally, examination of liver sections of the recovery group stained with Mallory’s trichrome stain, showed very slight rise in quantity of collagen fibers around central veins, blood sinusoids as well as around and in-between components of portal tracts with cytoplasmic small vacuoles and pyknotic nuclei. Furthermore, examination of PAS-stained liver sections obtained from this group showed moderate glycogen content in the hepatocytes at portal and central areas "figure 2E and 2F".

The results observed in table-4 and chart-4 showed non-significant rise of collagen area in the liver tissue of obese group when compared with the control group, there was also non-significant reduction of collagen area in the liver tissue of recovery group when compared to the obese group.

**Table (4):** Comparison between the median values, P values and inter-quartile ranges of collagen percentage area among hepatocytes (detected by Mallory’s trichrome stain) in various groups.

| Group    | Median of Collagen area % |                     |
|----------|---------------------------|---------------------|
|          | Median                    | Interquartile range |
| Control  | 1.80 <sup>a</sup>         | 2.45                |
| Obese    | 2.33 <sup>a</sup>         | 3.77                |
| Recovery | 1.85 <sup>a</sup>         | 3.51                |

Groups with variation superscript vary significantly (P<0.05).

(a) High value - (d) Low value - (b) and (c) In between. Analysis and comparisons based on non-parametric methods.

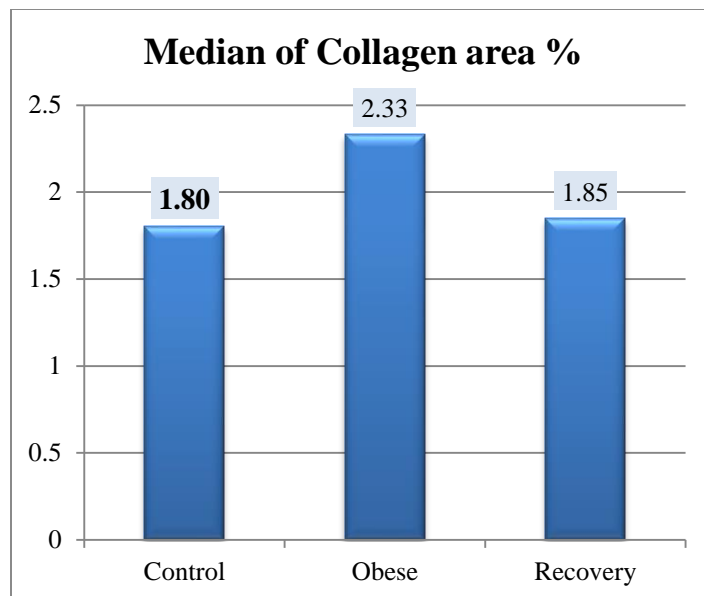


**Chart (4):** Comparison of the median values of collagen area percentages among hepatocytes (detected by Mallory trichrome stain) in different groups

There was also a highly significant reduction in the optical density of glycogen in the obese group when compared to the control group. There was also a significant rise in the optical density of glycogen in the recovery group when compared to the obese group, however, the optical density in the recovery group was lower than that of the control group (table-5 and chart-5).

**Table (5):** Comparison of the median values, P values and inter-quartile range of optical densities of glycogen in the hepatocytes in various groups (detected by PAS stain).

| Group    | Median of Optical density |                     |
|----------|---------------------------|---------------------|
|          | Median                    | Interquartile range |
| Control  | 0.241 <sup>a</sup>        | 0.057               |
| Obese    | 0.138 <sup>c</sup>        | 0.021               |
| Recovery | 0.205 <sup>b</sup>        | 0.018               |

Groups with variation superscript vary significantly (P<0.05).

(a) High value - (d) Low value - (b) and (c) In between. Analysis and comparisons based on non-parametric methods.

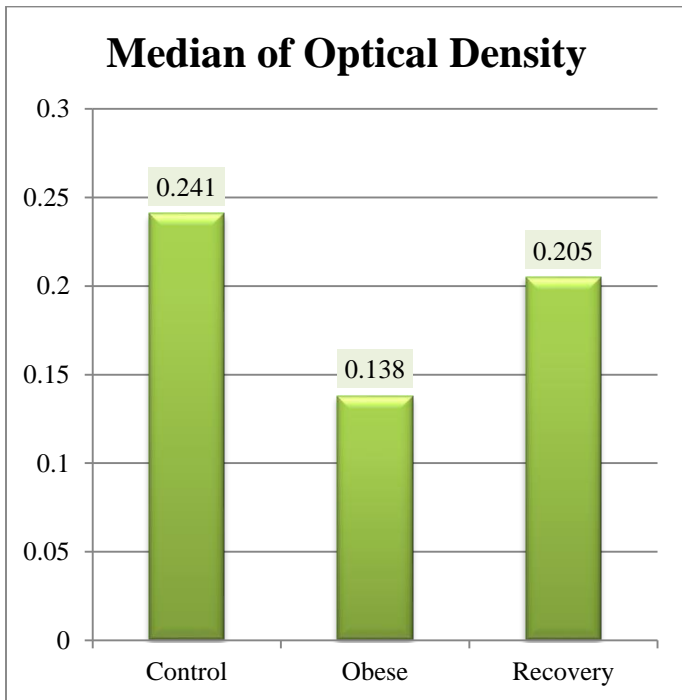


**Chart (5):** Comparison between the median values of optical densities of glycogen in the hepatocytes (detected by PAS stain) in different groups

**Electron microscopic results:**

Examination of ultrathin liver sections of the control group showed polyhedral hepatocytes containing rounded nuclei with prominent nucleoli and distinct nuclear envelope. Aggregations of euchromatin and heterochromatin granules were seen in the nuclei. The hepatocyte cytoplasm contained abundant cell organelles, mainly mitochondria of variable in size, rounded or oval with well-developed cristae. The mitochondria were found throughout the cytoplasm together with endoplasmic reticulum and secondary lysosomes. The

glycogen appeared as electron dense particles. Kupffer cells with their distinctive nuclei were found in Disse' spaces between the hepatocytes and the blood sinusoids "figure 3A and 3B".

Furthermore, ultrathin liver sections of obese group showed swelling of some hepatocytes and compression of their nuclei. Most of the hepatocyte nuclei were irregular, with condensed chromatin, indentation and widening of perinuclear space. Dilatation of small stacks of fragmented rough endoplasmic reticulum cisternae were seen in association with lysosomes. The mitochondria showed enlargement, swelling with complete or partial destruction of their cristae and most of them were surrounded by vacuoles. The endothelial cells showed hypertrophy while Von Kupffer cells contained many RBCs, and membranous vacuoles. The Disse spaces were dilated and contained fragments of distorted microvilli "figure 3C and 3D".

However, examination of ultrathin liver sections of the recovery group showed mild changes. Moderate ultrastructural changes were seen in the hepatocytes in the form of intracytoplasmic globules of various sizes (possibly lipids), primary and secondary lysosomes. The nuclei showed irregular nuclear membranes, condensed chromatin and widening of the perinuclear space. The mitochondria showed mild changes in the form of enlargement and swelling. Some mitochondria preserved their cristae; others showed destruction in their cristae. The Disse spaces of this group appeared dilated with moderate destruction of microvilli. Blood sinusoids showed moderate hypertrophic Von Kupffer cells that contained multiple membranous vacuoles (possibly lipids), and irregular condensed nuclei compressed by adjacent vacuoles "figure 3E and 3F".

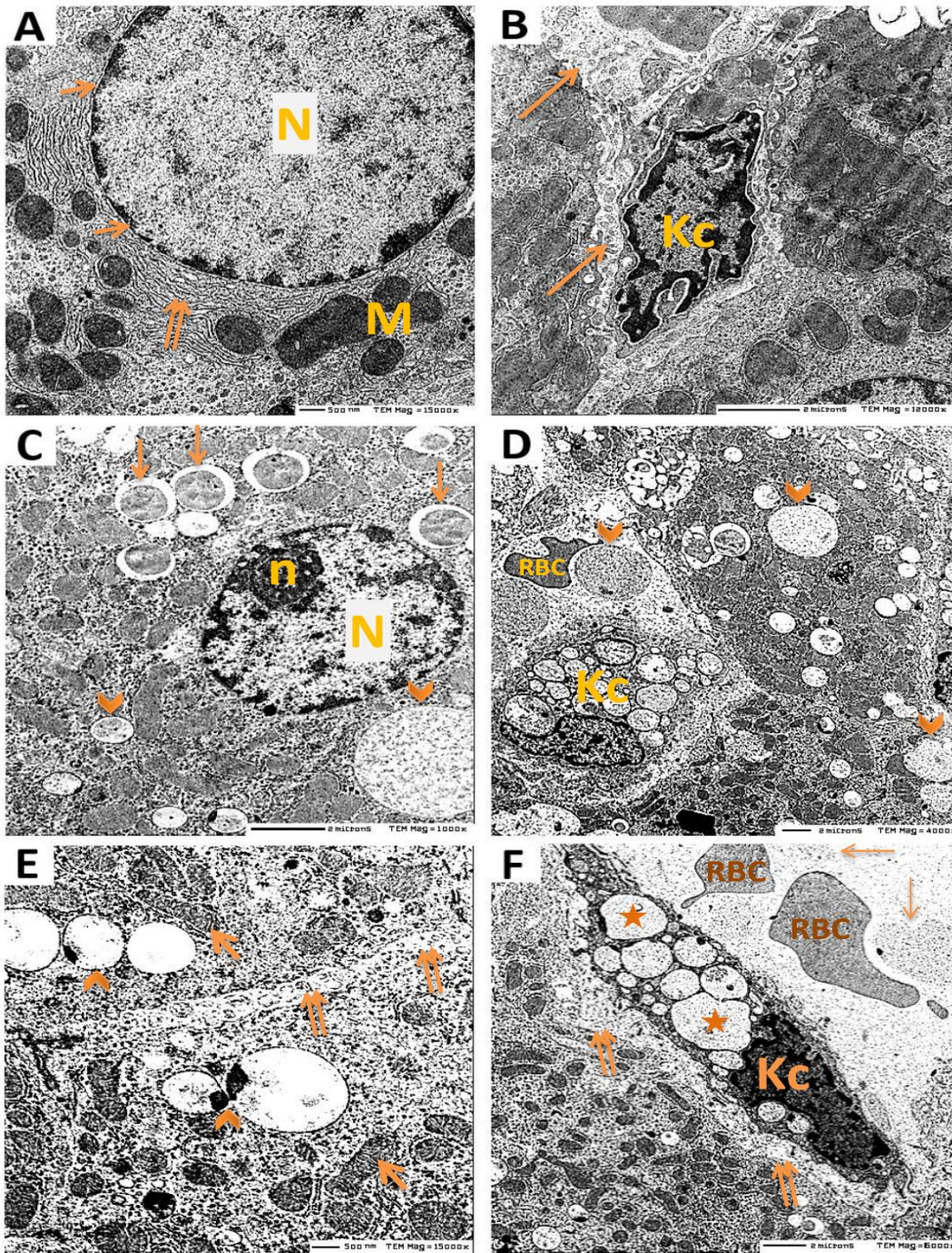


**Figure (3):** Electron micrographs of liver cells. (A): EM of hepatocyte from control group demonstrated normal ultrastructure of nucleus "N" and nuclear membrane "short arrows" that contained nuclear pores. There were clearly visible rough endoplasmic reticulum "double arrow" and mitochondria "M" (15000x). (B): EM of liver cells from control group showed space of Disse "long arrows" between hepatocytes and Kupffer cell "Kc" (12000x). (C): EM of hepatocyte from obese group demonstrated nucleus "N" with apparent nucleolus "n" and condensed chromatin. Some mitochondria were surrounded by vacuoles "arrows". Several vacuoles with variable size and shape are also seen within hepatocyte's cytoplasm "arrow heads" (10000x). (D): EM of liver cells from obese group showed enlarged highly disturbed Kupffer cell "Kc" with irregular and aggregations of small vacuoles. Several large vacuoles with variable size and shape were also seen within blood sinusoids and hepatocyte's cytoplasm "arrow heads" (4000x). (E): EM of hepatocyte from recovery group demonstrated variable sized mitochondria with cristae "thick arrows". Secondary lysosome "arrow heads" and space of Disse with disturbed microvilli "double arrows" were also seen. (15000x). (F): EM of hepatocyte from recovery group showed dilated space of Disse "double arrows" and blood sinusoid contained two large vacuoles "thin arrows" between RBCs while Kupffer cell "Kc" is enlarged containing aggregation of vacuoles "stars" (possibly lipids) (6000x).

## DISCUSSION

Obesity is a disorder characterized by chronic energy imbalance, whereby energy expenditure is consistently lower than energy intake, leading to the expansion of adipose tissue to allow the storage of excess energy<sup>(12)</sup>. Obesity is increasing in prevalence at a fast rate due to the rapidly increasing adoption of diets rich in saturated fats and simple carbohydrates, in combination with a sedentary lifestyle<sup>(13)</sup>. Obesity is linked to range of liver diseases recognized as nonalcoholic fatty liver disease, which is defined by rise in triglyceride content in hepatocytes with or without inflammation or fibrosis. Due to its higher incidence, the prospective advancement to severe liver disease and connection with serious metabolic diseases such as type-2 diabetes mellitus and coronary heart disease, nonalcoholic fatty liver disease has become a major public health problem<sup>(14)</sup>.

The pathogenesis of nonalcoholic fatty liver disease (NAFLD) and nonalcoholic steatohepatitis (NASH) remains unknown. It was described as long-term overnutrition, which causes aggregation of free fatty acids and triglycerides in the liver. The advancement of NAFLD to NASH, is connected with mitochondrial injury, oxidative stress, fatty acid lipotoxicity, inflammatory cytokines and innate immunity. Steatosis is the histological feature of NAFLD caused by high fatty acid influx and low fatty acid utilization in the hepatocytes<sup>(15)</sup>.

The goal of this research was to study the light and electron microscopic changes, as well as, the enzymatic activity of the liver after Triton-induced obesity in albino rats. We have used the rat model in this study because of great similarity and homology among genes of humans and rodents. In addition, Animals allow us to get answers quickly because ten days in life of rat is equivalent to one year in human terms<sup>(16)</sup>. Moreover, the Sprague-Dawley and Wistar rats are famous strains for studying obesity because they gain weight quickly<sup>(17)</sup>.

Our results revealed that there was highly significant increase in the body weight, liver weight and liver enzymes of rats in the obese group when compared to the control group; this may be due to lipid deposition in hepatocytes. These outcomes agree with those of *Ferguson et al.*<sup>(18)</sup> who reported that one of the major mechanisms of obesity is adipose tissue hyperplasia (increase in number of adipocytes) due to increased adipogenesis. Adipogenesis is a process by which pre-adipocytes become adipocytes. Furthermore, our findings coincide with those of *Cui et al.*<sup>(19)</sup> who mentioned that the liver weight in hyperlipidemic organisms was

greater than that of the normal diet group. He explained this by the presence of predominant microvesicular and focal macrovesicular fatty changes. This also explains the presence of significant improvement in the body weight and liver weight of the recovery group when compared with the obese group.

Moreover, the increase of liver enzymes were explained by *Noha et al.*<sup>(20)</sup> who stated that intravenous injection of Triton WR 1339 caused fat infiltration in hepatocytes which is responsible for their damage and the high levels of liver enzymes (AST and ALT). The increased fat concentration in hepatocytes can cause hepatocellular destruction directly through cellular cytotoxicity mediated by oxidative stress, mitochondrial impairment, free fatty acids, cytokine-induced hepatotoxicity and lipid peroxidation, all of which can cause liver dysfunction<sup>(21)</sup>. This also explains the presence of significant reduction in liver enzymes (ALT, AST and GGT) of the recovery group when compared with the obese group.

Light microscopic study showed many histological changes in the liver tissues; however, these changes are more prominent in the obese group. These changes include vacuolated hepatocytes with abnormal droplets (possibly fat). The hepatic portal areas had lost their normal structure and were filled with twisted blood vessels and bile canaliculi. These finding are explained by *Brunt and Tiniakos*<sup>(22)</sup> who noted that fat cells in fatty liver are active cells and secrete multiple immune modulator factors such as interleukin-6, pro-inflammatory cytokines, reactive oxygen species and tumor necrotic factor, all of which are related to chronic inflammatory process and hepatocyte injury. In the portal area, marked lymphocytic infiltration and hemolyzed RBCs were found.

There was also a non-significant increase of collagen area in the liver tissue of the obese group and the recovery group when compared with the control group. Collagen fibers were observed more around the hepatocytes and the walls of blood vessels leading to hepatocellular injury. These results were explained by *Horn et al.*<sup>(23)</sup> who stated that collagen in perisinusoidal spaces may influence blood supply to hepatocytes and decrease metabolite exchanges, resulting in hepatocellular injury and necrosis. However, there was a highly significant reduction in the optical density of glycogen in the obese group when compared to the control group. There was also a significant rise in the optical density of glycogen in the recovery group when compared to the obese group. However, the optical density in the

recovery group was lower than that of the control group. These findings agree with those of *Han et al.* (24) who reported highly affected glycogen content in the hepatocytes of the obese group and explained this by changed insulin levels, insulin sensitivity, and insulin resistance due to obesity.

The electron microscopic study showed many ultrastructural changes in the form of vacuoles or inclusions in the hepatocytes of the obese group and the recovery group. Some inclusions appeared as macrovesicular structures pushing the nucleus to the periphery giving distinguishing signet ring cell appearance. Other inclusions appeared as microvesicular vacuoles around central nucleus. Some mitochondria were engulfed by lysosomes. Large vacuoles were also observed within Kupffer cell possibly due to hyperlipidemia. These results agree with *Brunt and Tiniakos* (22) who reported vacuolations in liver cells forming microvesicular and macrovesicular steatosis. Macrovesicular steatosis is defined as abnormalities in the lipid synthesis, metabolism, and consumption. Microtubular disruption and severe cell injury can cause ballooned hepatocytes. The hallmark of liver disease, “microvesicular steatosis”, is connected to defective  $\beta$ -oxidation of fatty acids, implying mitochondrial abnormality (25). The cytoplasmic vacuolations were linked to lipid peroxidation since oxidative stress damages cell membranes in addition to the membranes of the cell organelles, increasing permeability and disrupting ion concentrations in the cytoplasm and cell organelles (26). The hepatocellular injury in obese group was possibly caused by 2 major mechanisms: direct cytotoxicity of fatty acids in hepatocytes as a result of increased intracellular fatty acid accumulation and/or indirect cytotoxicity of fatty acid lipid peroxidation (27).

We also detected small and shrunken nuclei with irregular torn nuclear membrane. Some of them showed alteration in chromatin distribution in the form of margination and clumping, this may be attributed to morphological injury in the nucleus due to obesity. The mitochondria of the obese group were disrupted, increased in size, with disrupted cristae, and their matrixes are of low density compared to the control group. These mitochondrial alterations were explained by *Weisberg et al.* (28) who stated that variations in the morphology of mitochondria in NAFLD, such as increased size, loss of cristae, and decreased matrix density, may be attributed to disruptions in the DNA and lipid oxidation. Obvious signs of improvement were detected in the liver tissue of recovery group. The space of Disse was dilated with few disturbed microvilli.

Kupffer cells were enlarged with aggregation of few vacuoles. Also, there was lymphocytic infiltration and hemolyzed RBCs. The hepatocytes showed normal histological shape with few vacuoles and many secondary lysosomes.

## CONCLUSION

The published results confirm that obesity is responsible for remarkable structural and functional abnormalities in the liver. The pathological changes involve the hepatocytes, and their glycogen content as well as the hepatic connective tissues. Obesity also induced inflammation of the hepatic tissues similar to steatosis or steatohepatitis.

## DECLARATIONS

- **Consent for Publication:** I verify that the author has agreed to submit the manuscript.
- **Availability of both data and material:** Available.
- **Competing interests:** None.
- **Funding:** None.
- **Conflicts of Interest:** The author declared that he had no conflicts of interest with regard to publication of this paper.

## REFERENCES

1. **Fried M, Yumuk V, Oppert J et al. (2013):** Interdisciplinary European Guidelines on metabolic and bariatric surgery. *Obes Facts*, 5: 449-68.
2. **WHO (2021):** Obesity and overweight. <https://www.who.int/news-room/fact-sheets/detail/obesity-and-overweight>
3. **Browning J, Horton J (2004):** Molecular mediators of hepatic steatosis and liver injury. *J Clin Invest*, 114: 147-152.
4. **Anthwal V, Ishaq F, Singh R et al. (2012):** Antioxidant and antiatherogenic impacts of *Catharanthus roseus* and *Hibiscus sabdariffa* on  $\text{Cu}^{++}$  mediated oxidation kinetics of low density lipoprotein. *Pelagia Research Library, Der Pharmacia Sinica*, 3 (4): 443-456
5. **Gholam P, Flancbaum L, Machan J et al. (2007):** Nonalcoholic fatty liver disease in severely obese subjects. *Am J Gastroenterol.*, 102: 399-408.
6. **Kleiner D, Brunt E, Van Natta M et al. (2005):** Design and validation of a histological scoring system for nonalcoholic fatty liver disease. *Hepatology*, 41: 1313-1321.
7. **National Research Council (2011):** Guide for the Care and Use of Laboratory Animals: Eighth Edition. Washington, DC: The National Academies Press. <https://doi.org/10.17226/12910>.
8. **Walaa A. Keshk and Saad A. Moeman (2015):** Impact of Chicory-Supplemented Diet on HMG-CoA Reductase, Acetyl-CoA Carboxylase, Visfatin and

- Anti-Oxidant Status in Triton WR-1339-Induced Hyperlipidemia. <https://doi.org/10.1111/jfbc.12115>.
9. **Woodard G (1965):** In *Methods of Animal Experimentation*, 1 (ed. W.J. Gay): 343–359. Academic Press, New York.
  10. **Mark W, Janet B, Eileen T et al. (2014):** Conventional transmission electron microscopy *Mol Biol Cell*, 25(3): 319–323.
  11. **Bancroft D, Marilyn G (2008):** *Theory and Practice of Histological Techniques*. 6th ed. Oxford: Churchill Livingstone Elsevier, 180: 168-174.
  12. **Ahn J, Lee H, Kim S et al. (2010):** Curcumin-induced suppression of adipogenic differentiation is accompanied by activation of Wnt/ $\beta$ -catenin signaling. *American Journal of Physiology-Cell Physiology*, 298:C1510-C1516.
  13. **McGill A (2014):** Causes of metabolic syndrome and obesity-related co-morbidities part 1. A composite unifying theory review of human-specific co-adaptations to brain energy consumption. <https://europepmc.org/article/MED/25708524>
  14. **Elisa F, Shelby S, Samuel K (2010):** Obesity and Nonalcoholic Fatty Liver Disease: Biochemical, Metabolic and Clinical Implications. *Center for Human Nutrition and Atkins Center of Excellence in Obesity Medicine, Published in final edited form as: Hepatology*, 51(2): 679–689.
  15. **Mahtab M, Fazle A (2013):** Non-alcoholic Fatty Liver Disease: A Review. *Journal of Gastroenterology and Hepatology Research*, 2(3):439–44.
  16. **Von Diemen V, Trindade E, Trindade M (2006):** Experimental model to induce obesity in rats. *Acta Cir Bras*, 21(6): 425-9.
  17. **Farley C, Cook J, Spar B et al. (2003):** Meal pattern analysis of diet-induced obesity in susceptible and resistant rats. *Obes Res.*, 11: 845-851.
  18. **Ferguson B, Nam H, Morrison R (2016):** Curcumin inhibits 3T3-L1 preadipocyte proliferation by mechanisms involving post-transcriptional p27 regulation. *Biochemistry and Biophysics Reports*, 5: 16-21.
  19. **Cui S, Xiao J, Jun W et al. (2011):** Effects of Lycium Barbarum Aqueous and Ethanol Extracts on High-Fat-Diet Induced Oxidative Stress in Rat Liver Tissue *Molecules*, 16: 9116-9128.
  20. **Noha M, Amal B, Abba M (2017):** Synergistic Cardioprotective Effects of Combined Chromium Picolinate and Atorvastatin Treatment in Triton X-100-Induced Hyperlipidemia in Rats: Impact on Some Biochemical Markers. *Biol Trace Elem Res.*, 180(2): 255–264.
  21. **Fabbrini E, Sullivan S, Klein S (2010):** Obesity and nonalcoholic fatty liver disease: biochemical, metabolic, and clinical implications. *Hepatology*, 51: 679-689.
  22. **Brunt E, Tiniakos D (2010):** Histopathology of nonalcoholic fatty liver disease. *World J Gastroenterol.*, 16(42): 5286-96.
  23. **Horn T, Jung J, Christoffersen P (1985):** Alcoholic liver injury: early changes of the Disse space in acinar zone. *Liver*, 6: 301-310.
  24. **Han S, Quon M, Kim J et al. (2007):** Adiponectin and cardiovascular disease: response to therapeutic interventions. *J. Am. Coll. Cardiol.*, 49: 531-538.
  25. **Tiniakos D, Kittas C (2005):** Pathology of nonalcoholic fatty liver disease. *Annals of gastroenterology*, 18(2): 148–59.
  26. **Panqueva R (2014):** Pathological aspects of fatty liver disease. *Rev Col Gastroenterol.*, 29(1):72–8.
  27. **Wierzbicki A, Oben J (2012):** Nonalcoholic fatty liver disease and lipids. *Curr Opin Lipidol.*, 23: 345–52.
  28. **Weisberg S, Leibel R, Tortoriello D (2008):** Dietary curcumin significantly improves obesity-associated inflammation and diabetes in mouse models of diabetes. *Endocrinology*, 149:3549–3558.